Long astral microtubules uncouple mitotic spindles from the cytokinetic furrow

Kathleen E. Rankin[1] and Linda Wordeman[1,2]

[1]Department of Physiology and Biophysics, University of Washington, Seattle, WA 98195
[2]Center for Cell Dynamics, Friday Harbor Laboratories, Friday Harbor, WA 98250

Astral microtubules (MTs) are known to be important for cleavage furrow induction and spindle positioning, and loss of astral MTs has been reported to increase cortical contractility. To investigate the effect of excess astral MT activity, we depleted the MT depolymerizer mitotic centromere-associated kinesin (MCAK) from HeLa cells to produce ultra-long, astral MTs during mitosis. MCAK depletion promoted dramatic spindle rocking in early anaphase, wherein the entire mitotic spindle oscillated along the spindle axis from one proto-daughter cell to the other, driven by oscillations of cortical nonmuscle myosin II. The effect was phenocopied by taxol treatment. Live imaging revealed that cortical actin partially vacates the polar cortex in favor of the equatorial cortex during anaphase. We propose that this renders the polar actin cortex vulnerable to rupture during normal contractile activity and that long astral MTs enlarge the blebs. Excessively large blebs displace mitotic spindle position by cytoplasmic flow, triggering the oscillations as the blebs resolve.

Introduction

The mitotic spindle directs the placement and assembly of the cleavage furrow and maintains the position of the chromosomes throughout furrow ingression and abscission during cytokinesis. Both astral and midzone microtubules (MTs) appear to contribute to the positioning of cleavage furrow components (Mishima et al., 2002; Werner et al., 2007; Foe and von Dassow, 2008), and in the absence of one structure, the other may suffice (Rieder et al., 1997; Alsop and Zhang, 2003; von Dassow et al., 2009). The role of contact between astral MTs and the cortex during cytokinesis is less clear. Some studies suggest that a subset of stable astral MTs may deliver cleavage furrow components to the central cortex to specify the cleavage furrow (Canman et al., 2003; Foe and von Dassow, 2008; Odell and Foe, 2008), whereas the bulk of the dynamic polar astral MTs inhibit furrowing at the poles. This is supported by experiments from several studies in which astral MTs were disrupted with nocodazole, inducing aberrant and excessive contractility in the cortex (Canman et al., 2000; Pletjushkina et al., 2001; Paluch et al., 2005; Murthy and Wadsworth, 2008).

Because loss of astral MTs increases cortical contractility, increasing the astral MT density or length may suppress contractility or, alternatively, lead to aberrant delivery of furrow components to the cortex. To test this hypothesis, we depleted MCAK from HeLa cells, which is known to lead to long astral MTs (Kline-Smith et al., 2004; Stout et al., 2006). In contrast to our expectations, MCAK depletion produced pronounced longitudinal spindle rocking after anaphase. We determined that oscillation of nonmuscle myosin II (hereafter myosin) between the polar cortices drives the spindle rocking, an effect that was phenocopied by treatment with the MT-stabilizing drug taxol. Rocking was correlated with polar blebs of unusually large size. Live imaging of cortical actin filaments during anaphase revealed that as equatorial actin polymer increases, polar actin polymer decreases proportionately. Thus, the polar actin cortex is preferentially weakened during cytokinesis, making it vulnerable to rupture. This study provides a mechanistic explanation for spindle oscillations, which can occur when MTs are hyperstabilized.

Results and discussion

MCAK depletion causes anaphase spindle rocking and cortical myosin oscillation

Transfection of a HeLa cell line stably expressing EGFP–α-tubulin with MCAK-specific siRNA results in 90% depletion

Correspondence to Linda Wordeman: worde@u.washington.edu

K.E. Rankin's present address is Bernhard Nocht Institute for Tropical Medicine, Hamburg 42818-404, Germany.

Abbreviations used in this paper: MT, microtubule.

© 2010 Rankin and Wordeman This article is distributed under the terms of an Attribution–Noncommercial–Share Alike–No Mirror Sites license for the first six months after the publication date (see http://www.rupress.org/terms). After six months it is available under a Creative Commons License (Attribution–Noncommercial–Share Alike 3.0 Unported license, as described at http://creativecommons.org/licenses/by-nc-sa/3.0/).

The Rockefeller University Press $30.00
J. Cell Biol. Vol. 190 No. 1 35–43
www.jcb.org/cgi/doi/10.1083/jcb.201004017

THE JOURNAL OF CELL BIOLOGY

Downloaded from http://rupress.org/jcb/article-pdf/190/1/35/1478393/jcb_201004017.pdf by guest on 05 December 2025

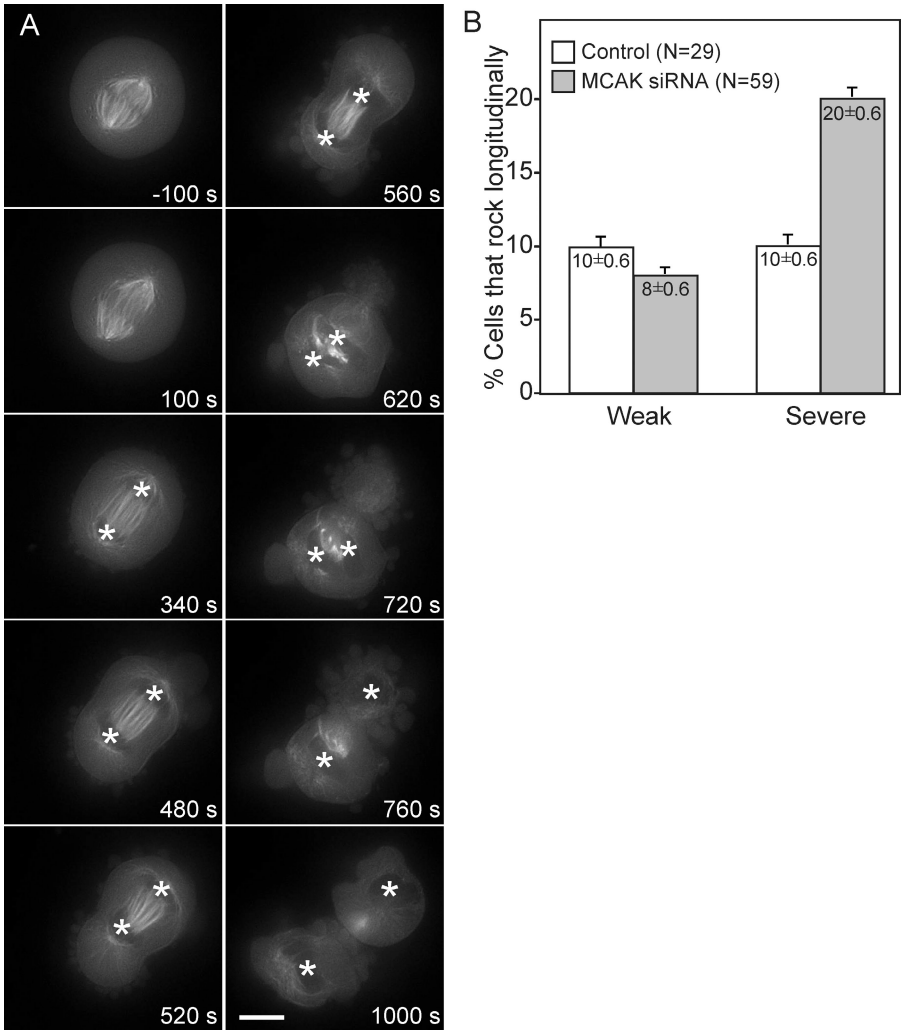

Figure 1. **MCAK depletion causes severe anaphase spindle rocking.** (A) A HeLa cell stably expressing EGFP–α-tubulin and treated with MCAK-specific siRNA for 36 h exhibiting severe spindle rocking. Time is relative to anaphase onset. Asterisks mark location of chromosomes. Bar, 5 µm. (B) Quantification of cells filmed exhibiting spindle rocking. MCAK depletions had significantly more severe spindle rocking than controls ($P < 0.0001$). Weak rocking was defined as movement of the spindle along the spindle axis without either set of chromosomes moving through the cleavage furrow. Severe spindle rocking was scored when the chromosomes moved through the cleavage furrow at least once. Error bars indicate SEM.

of MCAK (Fig. S1 A). Unexpectedly, some cells depleted of MCAK exhibited dramatic spindle rocking in early anaphase in which the entire spindle and both sets of chromosomes oscillated along the spindle axis between proto-daughter cells (Fig. 1 A and Video 1). Spindle rocking was binned by severity and compared with control siRNA-transfected cells (Fig. 1 B; and Videos 1 and 2). Severe rocking consisted of longitudinal oscillations in which the chromosomes moved through the cleavage furrow (Fig. 1 A and Video 1) and resulted in failure of cytokinesis in 25–30% of cells (Fig. S1 B). Weakly rocking spindles exhibited longitudinal spindle movement without either set of chromosomes moving through the cleavage furrow and always completed cytokinesis with correct chromosome segregation. Of the parameters we measured, only severe rocking was correlated with MCAK depletion (Fig. 1 B; and Fig. S1, B–D). Interestingly, the spindle rocking resembled that which has been described previously in anillin-depleted cells (Straight et al., 2005; Zhao and Fang, 2005a) with the exception that the cleavage furrow ultimately completes cytokinesis.

To determine what drives anaphase spindle rocking, we imaged HeLa cells coexpressing EGFP–myosin IIA and mCherry–α-tubulin and either control siRNA (Video 3) or siRNA directed against MCAK (Video 4). In cells with severe rocking, myosin accumulates at the cleavage furrow and the polar cortex after initial chromosome segregation and then proceeds to oscillate between each polar cortex as the spindle is oscillating (Fig. 2 A and Video 4), indicating that it drives the rocking. To confirm this, we treated cells with the ROCK inhibitor Y-27632 to inhibit cortical contractile activity. This treatment abolished longitudinal rocking but not dynein-dependent lateral oscillations (Fig. S2, A and B).

Kymographs along the spindle axis of live cells (Fig. 2 B, schematic) showed that the onset of spindle rocking was often correlated with breaks (blebs) in the cortical myosin (Fig. 2 C, arrows), leading to proximal flow of the spindle into the bleb (Fig. 2 C, right). Resolution of the bleb by reassembly and contraction of myosin shifts the entire spindle and chromosomes to the other side of the cell. As the spindle moves to the other side of the cell under the power of the contracting myosin, blebs form on the opposite polar cortex, initiating the process again. Out of phase oscillations continue until the cleavage furrow closes. In severely affected cells, the cleavage furrow may trap both daughter nuclei in one cell (Fig. S1 B).

Downloaded from http://rupress.org/jcb/article-pdf/190/1/35/1478393/jcb_201004017.pdf by guest on 05 December 2025

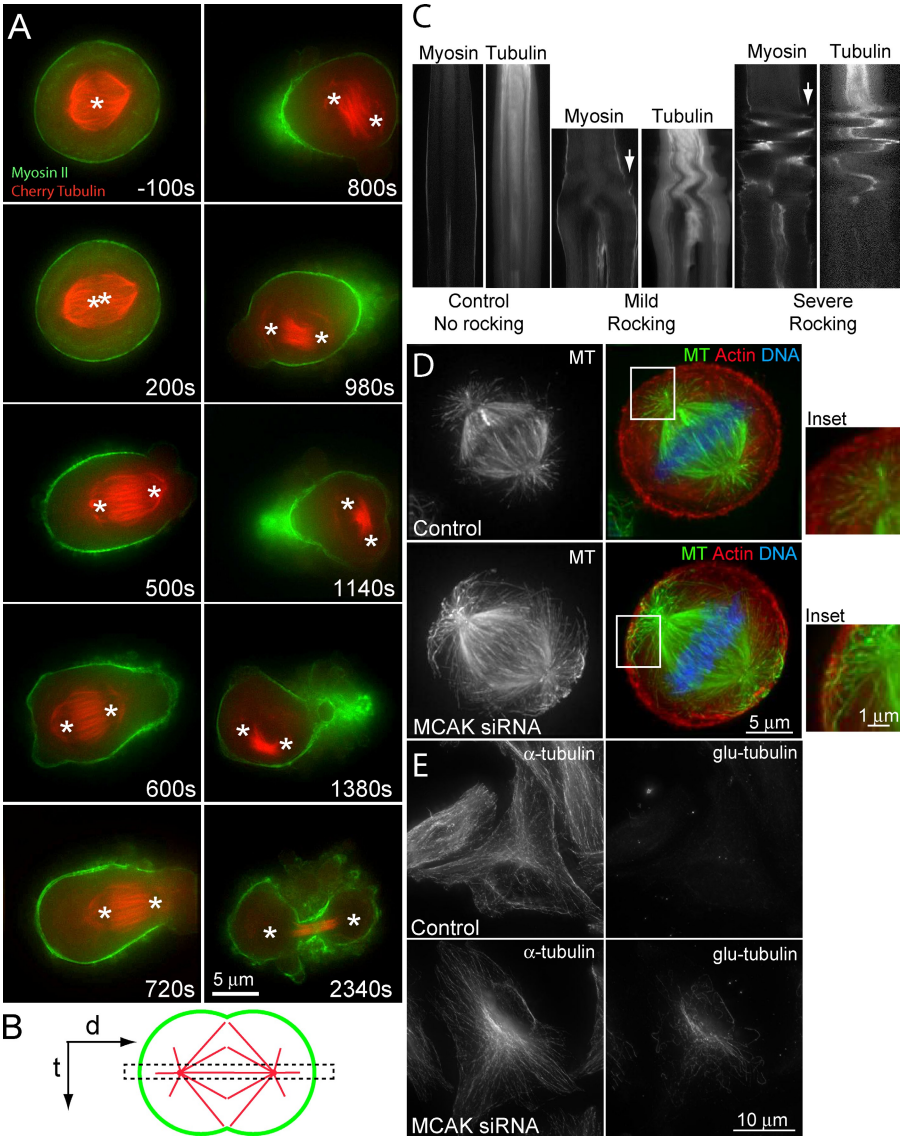

Figure 2. **Severe spindle rocking is driven by cortical myosin and long astral MTs.** (A) Still images from Video 4 showing spindle oscillations in a HeLa cell expressing EGFP–myosin IIA (green) and mCherry–α-tubulin (red) and treated with MCAK-specific siRNA for 36 h. Asterisks mark the location of chromosomes. Time is relative to anaphase onset. (B) A schematic of kymographs in C is shown. The dashed box indicates the slice plane for the construction of the kymographs. d, distance; t, time. (C) Kymographs of cells in anaphase with normal (left), weak (middle), and severe (right) rocking. Arrows indicate bleb and subsequent movement of the spindle. (D) Astral MTs are longer in metaphase HeLa cells treated with MCAK-specific siRNA for 48 h (bottom) relative to control cells (top). MTs are labeled with anti–α-tubulin (green), actin filaments with Texas red phalloidin (red), and DNA with DAPI (blue). Insets show magnified views of boxed regions. (E) MT stability increases in interphase when MCAK is depleted, as indicated by staining with anti–Glu-tubulin antibodies (right) after treatment with control (top) and MCAK-specific siRNA (bottom) for 48 h.

MCAK depletion causes long astral MTs and increases MT stability

If myosin drives the spindle oscillations, then why does the depletion of an MT depolymerizer promote this activity? Cells depleted of MCAK exhibited long astral MTs that interdigitate with the actin cortex in both metaphase and anaphase compared with control cells (Fig. 2 D and Fig. S3 A). In interphase cells, MCAK siRNA treatment leads to an increase in the amount of Glu-tubulin (Fig. 2 E), a detyrosinated form of tubulin that is an established marker for stable MTs (Gundersen et al., 1987), indicating that MCAK depletion increases MT stability.

The spindle rocking driven by myosin could be triggered by increased cortical delivery of RhoA activators by astral MTs (Canman et al., 2000; Rogers et al., 2004) or, alternatively, by altering the mechanical interaction of stable astral MTs with the cortex (Kozlowski et al., 2007). To investigate the first hypothesis, we quantified EB1 and phosphorylated myosin in the cortex of MCAK-depleted and control cells. EB1 has been implicated in RhoA activation (Rogers et al., 2004) and is known to interact with MCAK (Mennella et al., 2005; Lee et al., 2008; Honnappa et al., 2009). Although MCAK-depleted cells did exhibit significantly more EB1 on astral MTs compared with control cells (Fig. S2 C), we saw no increase in active (phosphorylated) myosin in MCAK-depleted cells as compared with controls (Fig. S2, D and E). Thus, it is unlikely that the increase in EB1 on astral MTs leads to an increased or ectopic cortical myosin activation.

Taxol treatment induces spindle rocking

Treating cells with the MT-stabilizing drug taxol is known to cause an increase in Glu-tubulin in interphase cells (Gundersen et al., 1987) and to alter astral MT stability (Shannon et al., 2005), similar to MCAK depletion. We applied 10 µM taxol to cells expressing EGFP–myosin IIA and mCherry–α-tubulin just after anaphase initiation. This treatment induced spindle oscillations remarkably similar to those seen in MCAK-depleted cells (Fig. 3, A and B; and Video 5).

Similar to MCAK depletion, astral MTs in control cells were short and primarily did not interact with the cortex (Fig. 3 C, top inset). In cells treated with 10 µM taxol for 1 min, the astral

Downloaded from http://rupress.org/jcb/article-pdf/190/1/35/1478393/jcb_201004017.pdf by guest on 05 December 2025

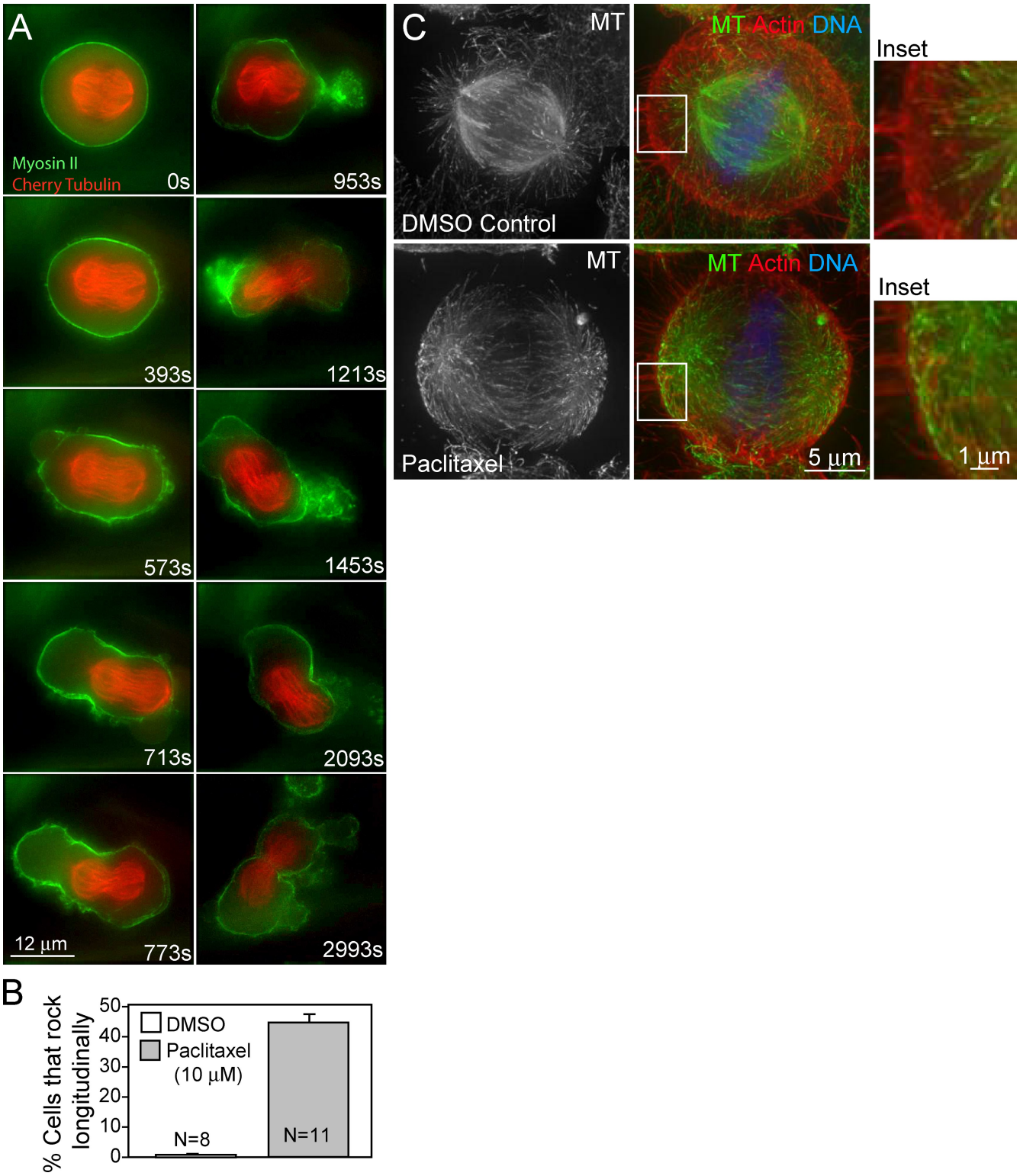

Figure 3. **Taxol treatment causes severe spindle rocking and long astral MTs.** (A) Representative HeLa cell coexpressing EGFP–myosin IIA and mCherry–α-tubulin with severe spindle rocking treated with 10 µM taxol added 80 s after anaphase onset. (B) 45 ± 2% of cells treated with 10 µM taxol exhibited spindle rocking compared with no DMSO-treated cells. (C) HeLa cells treated with 10 µM taxol for 1 min have longer astral MTs than cells treated with DMSO. Astral MTs in DMSO-treated cells do not contact the cortex (top inset), whereas MTs in taxol-treated cells come in close contact with the cortex (bottom inset). Insets show higher magnification views of boxed areas. Error bars indicate SEM.

MTs were much longer (Fig. 3 C, bottom inset). Similar results were seen in anaphase where astral MTs were much longer in both MCAK-depleted and taxol- treated cells (Fig. S3).

Quantification of EB1 on astral MTs in taxol-treated cells showed a slight decrease in astral EB1 staining compared with DMSO-treated cells (unpublished data), further refuting the idea

Downloaded from http://rupress.org/jcb/article-pdf/190/1/35/1478393/jcb_201004017.pdf by guest on 05 December 2025

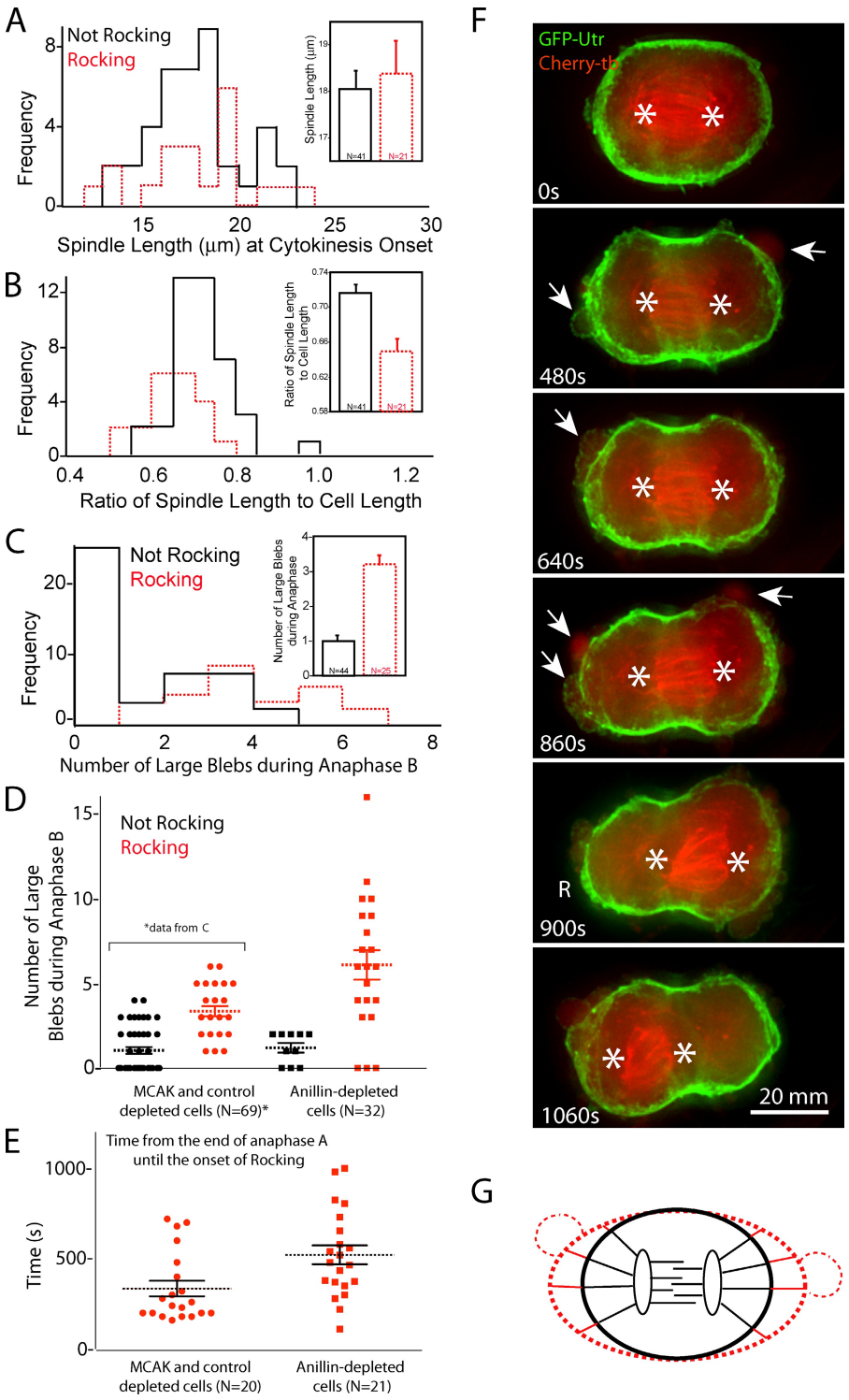

Figure 4. **Spindle rocking is correlated with large blebs.** (A) There is no correlation between spindle length at cytokinesis onset and spindle rocking. (B) Increased cell length correlates with spindle rocking. (C) Spindle rocking is correlated with greater numbers of blebs of diameter ≥1 μm ($P < 0.0001$). (D) Increased numbers of large blebs correlate with rocking in anillin siRNA-treated cells ($P < 0.0008$). (E) There is a modest but significant difference in the time it takes for cells to begin rocking in anillin siRNA-treated cells versus MCAK siRNA-treated cells ($P = 0.007$). (D and E) Dotted lines indicate the mean. (F) The onset of rocking in a live HeLa cell treated with siRNA directed against anillin and coexpressing mCherry–α-tubulin (red) and GFP-Utr (green) is shown. Large blebs are indicated (arrows). Resolution (R) of a particularly large bleb precedes the onset of rocking. Asterisks indicate DNA. (G) Diagram summarizing the features (cell length and large blebs) in red that are associated with spindle rocking. Error bars indicate SEM.

that long astral MTs globally increase myosin activation in the cortex via an EB1-bound RhoA activator. Instead, it is more likely that increased stabilization of astral MTs is directly correlated with spindle oscillations.

Spindle rocking is strongly correlated with large blebs of the polar cortex

To pinpoint mechanistically the trigger for spindle rocking, we binned our live imaging data into two groups, rocking and not rocking, and quantified cellular parameters correlated with rocking. We found that there was no significant difference between the lengths of the spindles at cytokinesis onset, which is the time at which most cells begin to rock (Fig. 4 A). In contrast, the cell length, measured from polar cortex to polar cortex, was significantly longer for cells that rock (Fig. 4 B). Thus, a lower ratio of spindle length to cell length is correlated with rocking spindles. We observed an even stronger correlation between large blebs (those ≥0.5 μm in diameter at their widest point) and spindle rocking (Fig. 4 C).

Downloaded from http://rupress.org/jcb/article-pdf/190/1/35/1478393/jcb_201004017.pdf by guest on 05 December 2025

Previously, spindle rocking has been correlated with anillin depletion (Straight et al., 2005; Zhao and Fang, 2005a). We examined anillin-depleted cells to determine whether rocking was correlated with large blebs. Two thirds of the cells in our anillin-depleted cells rock as compared with 10 ± 2% of control cells transfected with empty pSUPER vector. We found that rocking in anillin-depleted cells was highly correlated with large blebs (Fig. 4 C). Because closure of the furrow is delayed during anillin depletion relative to MCAK depletion, we scored the time to the onset of rocking in anillin-depleted cells versus cells depleted with MCAK. We found a modest but significant increase in the time it takes for anillin-depleted cells to begin rocking (Fig. 4 E). This is likely the explanation for why the number of blebs in rocking anillin-depleted cells is high relative to rocking MCAK-depleted cells (Fig. 4 D). Anillin-depleted cells are delayed in cytokinesis precisely at the time when blebbing is maximal. At this time, every bleb is potentially risky even if the level of MT polymer is normal. An anillin-depleted cell expressing GFP-Utr to visualize actin filaments (Burkel et al., 2007) and mCherry–α-tubulin is shown in Fig. 4 F. Large blebs (Fig. 4 F, arrows) form and resolve, eventually leading to spindle rocking. The parameters consistent with rocking spindles are outlined in Fig. 4 G (red). Large blebs promote cytoplasmic flow sufficient to pull the spindle away from the establishing cleavage furrow.

Polar cortical actin is decreased during anaphase relative to metaphase

To visualize the interaction of polymerizing MTs with the actin cortex, we imaged cells expressing GFP-Utr (Burkel et al., 2007) and mRFP-EB3. Surprisingly, when we quantified cortical filamentous actin fluorescence, we found that the polar actin decreased proportionally during anaphase as the equatorial actin increased in preparation for cytokinesis (Fig. 5, A and B). Although it is not surprising that actin increases equatorially, it was interesting to observe that polar actin decreased proportionately. We propose that loss of polar cortical actin renders the polar cortex more prone to blebbing during anaphase. Some amount of blebbing is a common occurrence during anaphase and cytokinesis. This process can be observed in the MCAK-depleted cell in Fig. 5 C, which goes on to rock longitudinally (Fig. 5, D and E; and Video 6). Because MTs continuously bombard the actin cortex in all cells without necessarily causing blebbing, we hypothesize that excess MT polymer does not trigger the bleb but, instead, invades a stochastically occurring bleb (Fig. 5 F), further widening the bleb and leading to cytoplasmic flow sufficiently forceful to displace the entire spindle from the cytokinetic furrow. Resolution of this "mega-bleb" via Rho-dependent myosin contraction (Charras et al., 2006) triggers the downstream oscillations. It has been established that MTs must be sufficiently dynamic for proper spindle positioning using dynein-dependent pulling forces (O'Connell and Wang, 2000; Nguyen-Ngoc et al., 2007). However, we have discovered another critical requirement for dynamic astral MTs during anaphase: suppression and minimization of cortical blebs. Bleb rupture can lead to forceful cytoplasmic flow, pulling the spindle away from the cytokinetic furrow. The normal process of resolution of such a large bleb (Charras et al., 2008), coupled with the displacement of the spindle midzone, hijacks the contractile machinery of the cortex away from the cytokinetic furrow. This leads to back and forth rocking of the spindle as the mega-blebs form and resolve on each end of the spindle with a slight temporal offset, possibly analogous to the traveling waves of cortical activity described as "circus waves" (Charras et al., 2008).

Treatments that delay cytokinetic furrowing (Straight et al., 2005; Zhao and Fang, 2005b; Cai et al., 2010) arrest the cell during this particularly dangerous time in the cell cycle when MT polymer is stabilizing and the cortex is vulnerable. Our data are relevant to anillin depletion in that they suggest a mechanism that leads to spindle rocking even when cytokinesis is not delayed, increasing the surface area of large blebs. We propose that several treatments that delay cytokinesis, weaken cortical actin, or stabilize MTs will compromise the polar cortex and promote hazardous spindle rocking. In this study, we provide mechanistic insight into the influence of bleb-dependent force generation on spindle positioning. Furthermore, we reveal a susceptible time during cytokinesis when regulation of astral MT length is of key importance in maintaining register between the mitotic spindle and the cleavage furrow.

Materials and methods

Cell culture and siRNA transfections

HeLa cells were cultured as previously described (Maney et al., 1998). HeLa cells were transfected with plasmid DNA by electroporation using the Nucleofector II (Lomax) according to the manufacturer's instructions. Cells were transfected with siRNA using transfection reagent (OligofectAMINE; Invitrogen) according to the manufacturer's instructions. For MCAK depletion, cells were transfected with 120 nM siRNA targeting the MCAK sequence 5′-GCAGGCUAGCAGACAAAU-3′ (Applied Biosystems). For control experiments, cells were transfected with 120 nM negative control siRNA1 (Applied Biosystems).

Immunofluorescence, deconvolution, and kymograph construction

HeLa cells were fixed using the following fixations for the indicated antibodies. EB1 (BD) and γ-tubulin (Sigma-Aldrich) were fixed in 1% PFA in ice-cold MeOH for 2 min; DM1α and Texas red–phalloidin were fixed in 0.25% glutaraldehyde and 0.05% Triton X-100 for 1 min followed by 1% glutaraldehyde for 10 min and postfixed for 45 min in $NaBH_4$, all in cytoskeletal buffer (Small et al., 1999); dynein 70.1 (Sigma-Aldrich) was fixed in MT-stabilizing buffer (Straight et al., 2005) for 10 min at 37°C before fixation in ice-cold MeOH for 3 min and overnight antibody incubation; Glu-tubulin (Millipore) was fixed in ice-cold MeOH for 10 min; and Shα-MCAK was produced as described previously (Moore et al., 2005) with various fixations and overnight antibody incubation. For taxol experiments, taxol was added to cells with a final concentration of 10 µM for 1 min just before fixation. Anti–mouse, anti–rabbit, and anti–sheep secondary antibodies conjugated to Alexa Fluor 488 or Alexa Fluor 568 (Invitrogen) at 2 µg/ml or fluorescein-conjugated µ-chain–specific secondary antibody (The Jackson Laboratory) at 1:50 was incubated for 1 h at room temperature. Stained cells were mounted in Vectashield with DAPI (Vector Laboratories). Cells were imaged on an upright microscope (Nikon) equipped with a charge-coupled device camera (Sensys) and a 60× 1.4 NA lens (Nikon) or a system equipped with a charge-coupled device camera (Deltavision; Applied Precision) and a 60× 1.4 NA lens (Olympus). Images were deconvolved using an image-processing workstation (Deltavision). The line-scan function in ImageJ (National Institutes of Health) was used to construct the kymographs.

DNA constructs and transfections

EGFP–myosin IIA (Wei and Adelstein, 2000) was provided by R. Adelstein (National Heart, Lung, and Blood Institute, Bethesda, MD). mCherry–α-tubulin was constructed as previously described (Shaner et al., 2004). HeLa cells were transfected with DNA by electroporation using Nucleofector II.

Downloaded from http://rupress.org/jcb/article-pdf/190/1/35/1478393/jcb_201004017.pdf by guest on 05 December 2025

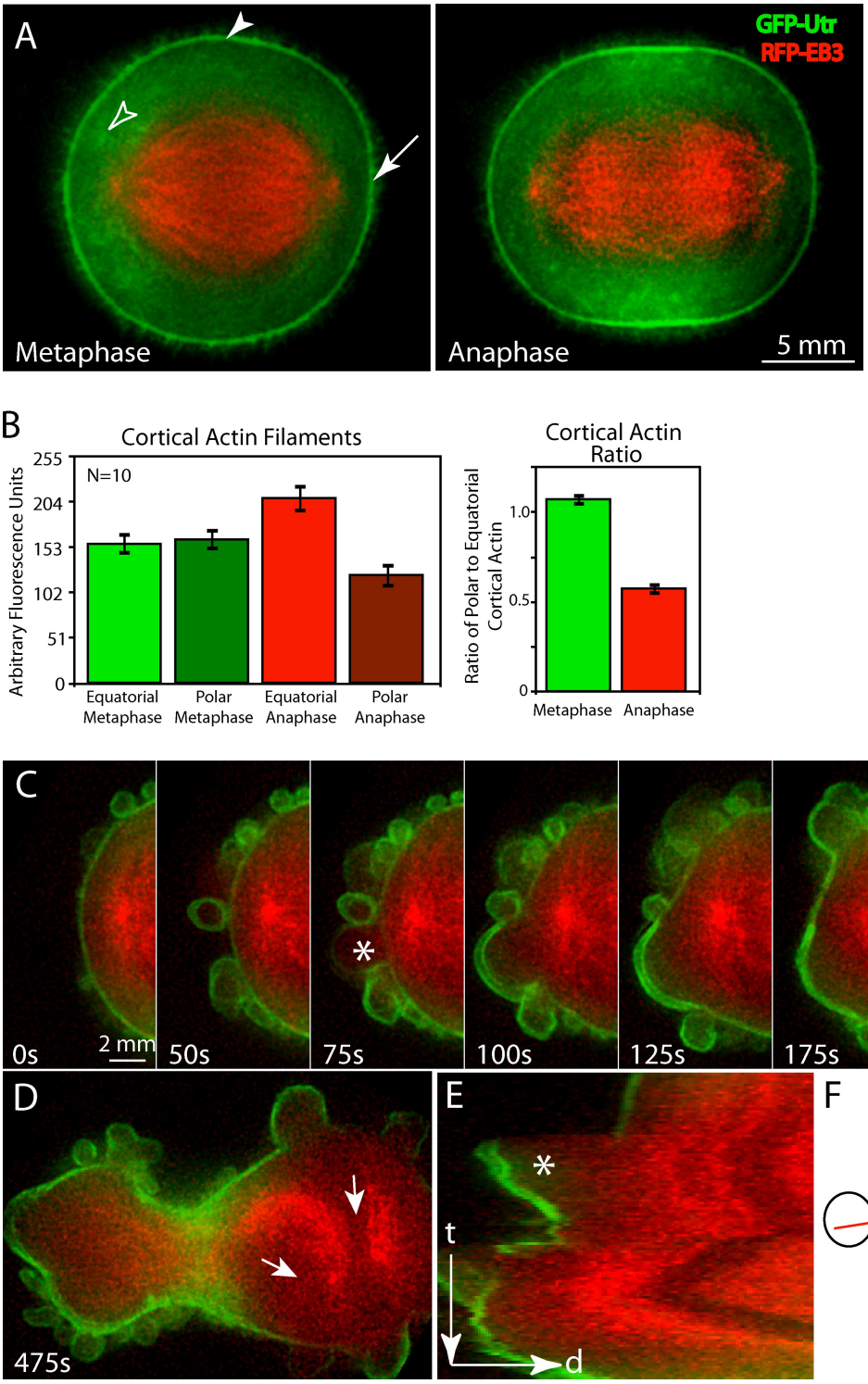

Figure 5. **The polar actin cortex is comparatively diminished during late anaphase.** (A) Live cell expressing GFP-Utr (green) and mRFP-EB3 (red) in metaphase (left) versus anaphase (right). The polar actin cortex (arrow), equatorial actin cortex (closed arrowhead), and deep actin filaments (open arrowhead) are indicated. (B) Quantification of polar versus equatorial cortical actin fluorescence (arbitrary units) in metaphase versus anaphase. Polar actin fluorescence decreases in parallel with an increase in equatorial actin before cytokinesis ($P < 0.0001$). (C) Successive frames of a live, MCAK-depleted cell expressing GFP-Utr and RFP-EB3. A bleb forms (asterisk), is invaded by MT ends, and widens. (D) The same cell at the onset of severe spindle rocking (arrows) is shown. (E) Kymograph of the same MCAK-depleted cell showing the temporal position of the first large bleb (asterisk). t, time; d, distance. (F) Diagram illustrating how blebs lead to rocking in MCAK-depleted cells. A small bleb forms (left) and is rapidly invaded with MT polymer, leading to a shift in the spindle position and an increase in the size of the bleb (middle). Resolution of the large bleb leads to a large reversal of the spindle position in the opposite direction (right). Error bars indicate SEM.

Downloaded from http://rupress.org/jcb/article-pdf/190/1/35/1478393/jcb_201004017.pdf by guest on 05 December 2025

SDS-PAGE and Western blotting

HeLa cells were lysed in 50 mM Tric-Cl, pH 8.0, 150 mM NaCl, 0.02% Na Azide, 0.1% SDS, 100 µg/ml PMSF, 1 µg/ml aprotinin, 1% NP-40, 0.5% deoxycholic acid (Na salt), 20 µg/ml DNaseI, and 5× EDTA-free protease inhibitor cocktail (Roche) for 48 h after transfection of siRNA. Lysates were clarified and separated on 4–12% acrylamide gradient gels by SDS-PAGE. Proteins were analyzed by Western blotting with polyclonal anti-MCAK antibodies and monoclonal anti-GAPDH antibodies (1:1,000; EMD). Bands were visualized by chemiluminescence, and signals were quantified with the gel analyzer function in ImageJ.

Live cell imaging

HeLa cells were cultured in MEMα medium (Life Technologies) with 10% FBS (Hyclone) at 37°C and 5% CO_2 on 35-mm glass coverslip dishes coated with poly-L-lysine (MatTek) for 48–72 h after DNA transfection and 36–48 h after siRNA transfection before analysis by time-lapse microscopy. Before filming, the cells were switched to 37°C CO_2-independent media (Life Technologies). Cells were imaged with a Deltavision RT system equipped with a CCD camera and a 60× 1.42 NA lens (Olympus) and a 37°C environmental chamber (Applied Precision). Z stacks containing three focal planes with 1.0 µm spacing were acquired at intervals of 20 s. For drug experiments, 10 mM taxol or an equal volume of DMSO was diluted in 1.0 ml 37°C CO_2-independent media for a concentration of 30 µM. This was added to the visualized cell plate containing 2 ml CO_2-independent media for a final taxol concentration of 10 µM.

Quantification of fixed and live images

To quantify the spindle length in MCAK-depleted cells, coverslips stained with anti–γ-tubulin antibodies were photographed, and only cells with both spindle poles in the same focal plane were analyzed. The distance between the two spindle poles was determined using ImageJ. To quantify the amount of astral EB1 and dynein in MCAK-depleted and taxol-treated cells, both astral areas of each cell (excluding the centrosomes) were encircled, and the mean background-subtracted intensity was measured. Cortical actin was quantified by recording the fluorescence at five points along the polar or equatorial cortex in metaphase and late anaphase (after the chromosomes have translocated all the way to the pole) and taking the mean of those points for the final value. Datasets were tested for significance with a two-tailed Mann Whitney test using Prism (version 5.0c; GraphPad Software, Inc.).

Online supplemental material

Fig. S1 shows the extent of MCAK knockdown by siRNA versus controls and that characteristics such as failure of DNA segregation, number of oscillations, and the frequency of those oscillations do not differ between severely rocking MCAK-depleted versus severely rocking control cells (which severely rock at a significantly lower frequency). Fig. S2 shows that inhibition of cortical contractility by Y-27632 eliminates rocking but does not disturb dynein-dependent lateral rocking and that astral EB1 is increased in MCAK-depleted cells, but cortical levels and distribution of phosphorylated myosin are not altered in MCAK-deleted or taxol-treated cells. Fig. S3 shows that anaphase astral MTs are significantly longer in MCAK-depleted or taxol-treated cells. Videos 1 and 2 show control siRNA and MCAK siRNA-treated cells, respectively. Videos 3 and 4 show control siRNA and MCAK siRNA-treated cells expressing GFP–myosin IIA and mCherry–α-tubulin, respectively. Video 5 shows a cell expressing GFP–myosin II and mCherry–α-tubulin that rocks after brief exposure to taxol. Video 6 shows a rocking anillin-depleted cell expressing Rfp-EB3 and GFP-Utr to label filamentous actin. Online supplemental material is available at http://www.jcb.org/cgi/content/full/jcb.201004017/DC1.

Mike Wagenbach provided excellent technical assistance. We thank Bill Bement (University of Wisconsin, Madison, WI) for the gift of GFP-Utr, Guowei Fang (Stanford University, Palo Alto, CA) for the gift of pSUPER-anillin, and Anna Akmanova (Erasmus University, Rotterdam, Netherlands) for the gift of mRFP-RB3. We are indebted to George von Dassow and Jason Stumpff for many significant discussions.

This study was supported by the National Institutes of Health (predoctoral training grant GM07270 to K.E. Rankin and grant GM69429 to L. Wordeman).

Submitted: 5 April 2010
Accepted: 9 June 2010

References

Alsop, G.B., and D. Zhang. 2003. Microtubules are the only structural constituent of the spindle apparatus required for induction of cell cleavage. *J. Cell Biol.* 162:383–390. doi:10.1083/jcb.200301073

Burkel, B.M., G. von Dassow, and W.M. Bement. 2007. Versatile fluorescent probes for actin filaments based on the actin-binding domain of utrophin. *Cell Motil. Cytoskeleton.* 64:822–832. doi:10.1002/cm.20226

Cai, S., L.N. Weaver, S.C. Ems-McClung, and C.E. Walczak. 2010. Proper organization of microtubule minus ends is needed for midzone stability and cytokinesis. *Curr. Biol.* 20:880–885. doi:10.1016/j.cub.2010.03.067

Canman, J.C., D.B. Hoffman, and E.D. Salmon. 2000. The role of pre- and post-anaphase microtubules in the cytokinesis phase of the cell cycle. *Curr. Biol.* 10:611–614. doi:10.1016/S0960-9822(00)00490-5

Canman, J.C., L.A. Cameron, P.S. Maddox, A. Straight, J.S. Tirnauer, T.J. Mitchison, G. Fang, T.M. Kapoor, and E.D. Salmon. 2003. Determining the position of the cell division plane. *Nature.* 424:1074–1078. doi:10.1038/nature01860

Charras, G.T., C.K. Hu, M. Coughlin, and T.J. Mitchison. 2006. Reassembly of contractile actin cortex in cell blebs. *J. Cell Biol.* 175:477–490. doi:10.1083/jcb.200602085

Charras, G.T., M. Coughlin, T.J. Mitchison, and L. Mahadevan. 2008. Life and times of a cellular bleb. *Biophys. J.* 94:1836–1853. doi:10.1529/biophysj.107.113605

Foe, V.E., and G. von Dassow. 2008. Stable and dynamic microtubules coordinately shape the myosin activation zone during cytokinetic furrow formation. *J. Cell Biol.* 183:457–470. doi:10.1083/jcb.200807128

Gundersen, G.G., S. Khawaja, and J.C. Bulinski. 1987. Postpolymerization detyrosination of alpha-tubulin: a mechanism for subcellular differentiation of microtubules. *J. Cell Biol.* 105:251–264. doi:10.1083/jcb.105.1.251

Honnappa, S., S.M. Gouveia, A. Weisbrich, F.F. Damberger, N.S. Bhavesh, H. Jawhari, I. Grigoriev, F.J. van Rijssel, R.M. Buey, A. Lawera, et al. 2009. An EB1-binding motif acts as a microtubule tip localization signal. *Cell.* 138:366–376. doi:10.1016/j.cell.2009.04.065

Kline-Smith, S.L., A. Khodjakov, P. Hergert, and C.E. Walczak. 2004. Depletion of centromeric MCAK leads to chromosome congression and segregation defects due to improper kinetochore attachments. *Mol. Biol. Cell.* 15:1146–1159. doi:10.1091/mbc.E03-08-0581

Kozlowski, C., M. Srayko, and F. Nedelec. 2007. Cortical microtubule contacts position the spindle in *C. elegans* embryos. *Cell.* 129:499–510. doi:10.1016/j.cell.2007.03.027

Lee, T., K.J. Langford, J.M. Askham, A. Brüning-Richardson, and E.E. Morrison. 2008. MCAK associates with EB1. *Oncogene.* 27:2494–2500. doi:10.1038/sj.onc.1210867

Maney, T., A.W. Hunter, M. Wagenbach, and L. Wordeman. 1998. Mitotic centromere-associated kinesin is important for anaphase chromosome segregation. *J. Cell Biol.* 142:787–801. doi:10.1083/jcb.142.3.787

Mennella, V., G.C. Rogers, S.L. Rogers, D.W. Buster, R.D. Vale, and D.J. Sharp. 2005. Functionally distinct kinesin-13 family members cooperate to regulate microtubule dynamics during interphase. *Nat. Cell Biol.* 7:235–245. doi:10.1038/ncb1222

Mishima, M., S. Kaitna, and M. Glotzer. 2002. Central spindle assembly and cytokinesis require a kinesin-like protein/RhoGAP complex with microtubule bundling activity. *Dev. Cell.* 2:41–54. doi:10.1016/S1534-5807(01)00110-1

Moore, A.T., K.E. Rankin, G. von Dassow, L. Peris, M. Wagenbach, Y. Ovechkina, A. Andrieux, D. Job, and L. Wordeman. 2005. MCAK associates with the tips of polymerizing microtubules. *J. Cell Biol.* 169:391–397. doi:10.1083/jcb.200411089

Murthy, K., and P. Wadsworth. 2008. Dual role for microtubules in regulating cortical contractility during cytokinesis. *J. Cell Sci.* 121:2350–2359. doi:10.1242/jcs.027052

Nguyen-Ngoc, T., K. Afshar, and P. Gönczy. 2007. Coupling of cortical dynein and G alpha proteins mediates spindle positioning in *Caenorhabditis elegans*. *Nat. Cell Biol.* 9:1294–1302. doi:10.1038/ncb1649

O'Connell, C.B., and Y.L. Wang. 2000. Mammalian spindle orientation and position respond to changes in cell shape in a dynein-dependent fashion. *Mol. Biol. Cell.* 11:1765–1774.

Odell, G.M., and V.E. Foe. 2008. An agent-based model contrasts opposite effects of dynamic and stable microtubules on cleavage furrow positioning. *J. Cell Biol.* 183:471–483. doi:10.1083/jcb.200807129

Paluch, E., M. Piel, J. Prost, M. Bornens, and C. Sykes. 2005. Cortical actomyosin breakage triggers shape oscillations in cells and cell fragments. *Biophys. J.* 89:724–733. doi:10.1529/biophysj.105.060590

Pletjushkina, O.J., Z. Rajfur, P. Pomorski, T.N. Oliver, J.M. Vasiliev, and K.A. Jacobson. 2001. Induction of cortical oscillations in spreading cells by depolymerization of microtubules. *Cell Motil. Cytoskeleton.* 48:235–244. doi:10.1002/cm.1012

Downloaded from http://rupress.org/jcb/article-pdf/190/1/35/1478393/jcb_201004017.pdf by guest on 05 December 2025

Rieder, C.L., A. Khodjakov, L.V. Paliulis, T.M. Fortier, R.W. Cole, and G. Sluder. 1997. Mitosis in vertebrate somatic cells with two spindles: implications for the metaphase/anaphase transition checkpoint and cleavage. *Proc. Natl. Acad. Sci. USA.* 94:5107–5112. doi:10.1073/pnas.94.10.5107

Rogers, S.L., U. Wiedemann, U. Häcker, C. Turck, and R.D. Vale. 2004. *Drosophila* RhoGEF2 associates with microtubule plus ends in an EB1-dependent manner. *Curr. Biol.* 14:1827–1833. doi:10.1016/j.cub.2004.09.078

Shaner, N.C., R.E. Campbell, P.A. Steinbach, B.N. Giepmans, A.E. Palmer, and R.Y. Tsien. 2004. Improved monomeric red, orange and yellow fluorescent proteins derived from *Discosoma sp.* red fluorescent protein. *Nat. Biotechnol.* 22:1567–1572. doi:10.1038/nbt1037

Shannon, K.B., J.C. Canman, C. Ben Moree, J.S. Tirnauer, and E.D. Salmon. 2005. Taxol-stabilized microtubules can position the cytokinetic furrow in mammalian cells. *Mol. Biol. Cell.* 16:4423–4436. doi:10.1091/mbc.E04-11-0974

Small, J.V., K. Rottner, P. Hahne, and K.I. Anderson. 1999. Visualising the actin cytoskeleton. *Microsc. Res. Tech.* 47:3–17. doi:10.1002/(SICI)1097-0029(19991001)47:1<3::AID-JEMT2>3.0.CO;2-2

Stout, J.R., R.S. Rizk, S.L. Kline, and C.E. Walczak. 2006. Deciphering protein function during mitosis in PtK cells using RNAi. *BMC Cell Biol.* 7:26. doi:10.1186/1471-2121-7-26

Straight, A.F., C.M. Field, and T.J. Mitchison. 2005. Anillin binds nonmuscle myosin II and regulates the contractile ring. *Mol. Biol. Cell.* 16:193–201. doi:10.1091/mbc.E04-08-0758

von Dassow, G., K.J. Verbrugghe, A.L. Miller, J.R. Sider, and W.M. Bement. 2009. Action at a distance during cytokinesis. *J. Cell Biol.* 187:831–845. doi:10.1083/jcb.200907090

Wei, Q., and R.S. Adelstein. 2000. Conditional expression of a truncated fragment of nonmuscle myosin II-A alters cell shape but not cytokinesis in HeLa cells. *Mol. Biol. Cell.* 11:3617–3627.

Werner, M., E. Munro, and M. Glotzer. 2007. Astral signals spatially bias cortical myosin recruitment to break symmetry and promote cytokinesis. *Curr. Biol.* 17:1286–1297. doi:10.1016/j.cub.2007.06.070

Zhao, W.M., and G. Fang. 2005a. Anillin is a substrate of anaphase-promoting complex/cyclosome (APC/C) that controls spatial contractility of myosin during late cytokinesis. *J. Biol. Chem.* 280:33516–33524. doi:10.1074/jbc.M504657200

Zhao, W.M., and G. Fang. 2005b. MgcRacGAP controls the assembly of the contractile ring and the initiation of cytokinesis. *Proc. Natl. Acad. Sci. USA.* 102:13158–13163. doi:10.1073/pnas.0504145102

Downloaded from http://rupress.org/jcb/article-pdf/190/1/35/1478393/jcb_201004017.pdf by guest on 05 December 2025